Progress In Electromagnetics Research, Vol. 138, 115–131, 2013

A FABRICATION OF INTELLIGENT SPIRAL RECONFIGURABLE BEAM FORMING ANTENNA FOR 2.35–2.39 GHz APPLICATIONS AND PATH LOSS MEASUREMENTS

Muzammil Jusoh[1, *], Mohd F. Jamlos[1], Muhammad R. Kamarudin[2], Thennarasan Sabapathy[1], Mohd I. Jais[1], and Mohd A. Jamlos[1]

[1]Advanced Communication Engineering Centre (ACE), School of Computer and Communication Engineering, Universiti Malaysia Perlis (UniMAP), Kampus Pauh Putra, Arau, Perlis 02600, Malaysia

[2]Wireless Communication Centre (WCC), Faculty of Electrical Engineering, Universiti Teknologi Malaysia, UTM Skudai, Johor 81310, Malaysia

Abstract—A reconfigurable beam forming antenna prototype using a spiral feed line is proposed in this paper. The presented antenna is integrated with PIN diode switches at a specific location of spiral feed line. It is discovered that the beam steering ability is greatly influenced by the spiral arm feed network. Four PIN diode switches have been incorporated at four different arms of spiral feed line to realize a beam forming ability. The intelligence behaviour of this antenna is conferred when the switches are connected to programmable intelligent computer (PIC) microcontroller. Certain configurations of PIC allow the antenna's radiation patterns to be adaptively changed within 0.01 ms. Therefore, the proposed antenna is capable of electronically forming the beam up to four different angles of $+176°$, $+10°$, $-1°$ and $-12°$. This antenna is small in size with 100 mm by 100 mm of substrate dimension. In this research, the site field antenna performance relying on the received signal strength (RSS) testing is tested intensively in Universiti Malaysia Perlis with varied distant points of line-of-sight (LOS) and non-line-of-sight (NLOS) propagation. With good simulation and measurement results, this antenna could be a promising candidate to be installed in applications such as a smart antenna system, cognitive radio, WiMAX and long term evolution (LTE).

Received 5 February 2013, Accepted 6 March 2013, Scheduled 16 March 2013

* Corresponding author: Muzammil Jusoh (ame_tango1@yahoo.com).

1. INTRODUCTION

Recently, the reconfigurable antenna has gained great attention among the researchers working on wireless communication system. Reconfigurable antenna can be divided into three categories; 1) frequency reconfigurable (performed for wideband and narrowband), 2) polarization reconfigurable (change in linear and circular polarization), and 3) radiation pattern reconfigurable (ability to shape and steer the antenna beam). This kind of antenna has the ability of performing more functions in a single antenna element than conventional antenna which is only capable of performing a single function in a single antenna. Therefore, this kind of antenna requires more than one antenna to perform multi-applications that eventually result in a complex and bulky system.

This research proposes a beam forming antenna functionality in a rich scattering wireless communication environment. A reconfigurable beam forming with the aptitude of positioning the main beam towards the wanted signal while suppressing the antenna beam in the direction of the unwanted signal is capable of mitigating fading and ensuring a spectrum efficiency with a minimum bit error rate (BER) [1]. Research on the reconfigurable microstrip antenna improved with integration of four PIN diode switches enables to achieve four distinguish steered angles. PIN diode switches have been widely integrated in a microstrip antenna for the reconfigurable purpose [2–6]. The PIN diode activation of ON and OFF states would then determine which part of the antenna will receive the radio frequency (RF) signal. In this research, these switches are controlled by the programmable intelligent computer (PIC) microcontroller with a 5 volt direct current (DC) supply.

This study proposes the use of an aperture coupled technique incorporated with PIN diode switches on the antenna feed line in order to reduce the signal degradation caused by the switches absorption. The spiral feeds network is introduced to reduce the antenna dimension and avoid overlap between the feed. This results in an optimum dimension and position of the spiral feed which has great influence in achieving beam forming functionality. There are a lot of effective studies on the microstrip antenna of the changes effect on reconfigurable ability in aperture coupled technique [7, 8].

The coarse-grained structure composed of two reflectors and a feeder is only capable of executing beam steering from -2° to $+2^\circ$ [9]. In [10], a beam covering off -70° to $+70^\circ$ has been achieved via a reconfigurable thin substrate antenna. A composite right/left-handed (CRLH) waveguide implemented in a substrate integrated waveguide (SIW) configuration is designed in [11]. This slot antenna exhibits a

wide range beam steering performance within -30° to $+30^\circ$. Though, the proposed antenna design has achieved beam forming characteristics at four signal directions of $+176^\circ$, $+10^\circ$, -1° and -12°.

To the authors' knowledge, none of the beam steering antennas achieved maximum beam at all beam steered direction [12–15]. In [13], a multi-feed dielectric resonator antenna has achieved beam steering of H-plane at 0° and 270° with peak gain of not exceed 2 dBi. However, the proposed antenna has successfully achieved a peak gain of 2.81 dBi, 4.2 dBi, 3.09 dBi and 3.89 dBi at each direction of $+176^\circ$, $+10^\circ$, -1° and -12°, respectively. It is observed that four rectangular radiating elements with different sizes, slots positioned and lengths of arm feed in a sequent spiral manner significantly contributes to the low spurious effect which eventually increases the antenna efficiency.

Other advantages of the proposed antenna lies in its size and cost effectiveness. With 100 mm by 100 mm in size, this antenna is considered small compared to the conventional microstrip antenna and could perform similar features to those in [14]. Moreover, the antenna performs well with minimum S_{11} of less than -10 dB, since the ultimate goal is to ensure that at least 90% of power is transmitted and only 10% of power reflected. With different switch configurations, the antenna functions well within operating frequencies of 2.35 to 2.41 GHz, which meets the WiMAX frequency dedicated to Packet One Sdn Bhd as regulated by the Malaysian Communication and Multimedia Commission (MCMC) as shown in Figure 1.

This paper is organized as follows. Section 2 explains the design of the proposed antenna via aperture coupled feed technique incorporates RF PIN diode switches. Such switching elements are controlled by PIC microcontroller. In Section 3, the comparison of measurement and simulation beam steering ability with different switch configurations at four spiral-arm feed is investigated. Moreover, the received power measurement of Agilent power sensor device is discussed. Finally, the conclusion is drawn in Section 4.

2. ANTENNA STRUCTURE

Figure 2 shows the antenna structure designed by competence 3D electromagnetic software, Computer Simulation Technology (CST). The proposed antenna is developed using an aperture coupled technique and consists of upper substrate and lower substrate. Generally, the aperture coupled feed has tough fabrication process since both substrate layers need to be aligned properly in order to obtain maximum power transfer from the feed to the radiating element and minimize the return loss. However, aperture coupled technique

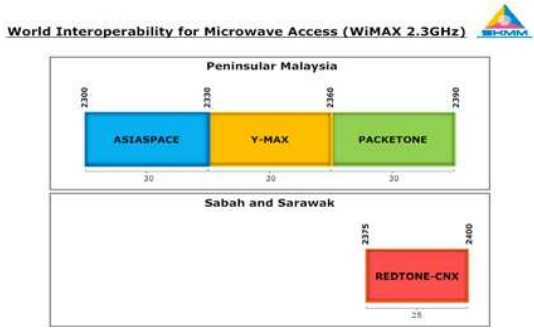

Figure 1. Malaysian WiMAX Spectrum Allocation Chart [8].

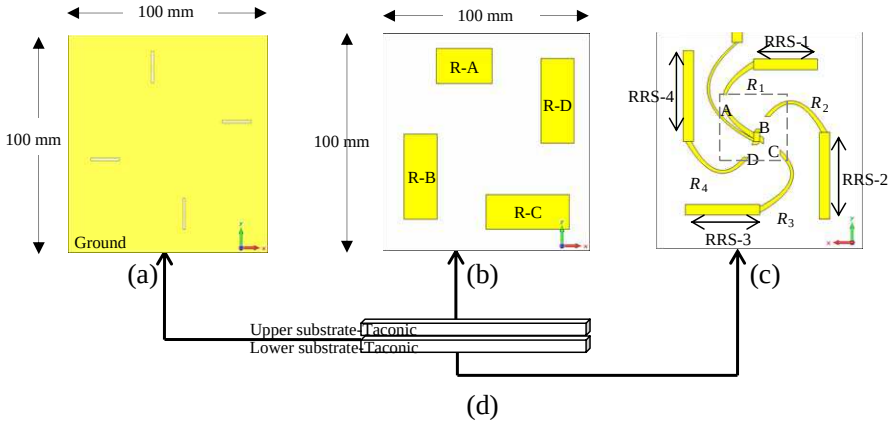

Figure 2. Geometry of the simulated antenna structure. (a) Rectangular slot aperture coupled. (b) Radiating element surface. (c) Spiral feed line. (d) Layout view.

enables the RF PIN diode switches to be incorporated at the feed line in providing the low spurious effect and increases the antenna efficiency. As shown in Figure 2(c), this antenna deploys four switches depicted as A, B, C and D at the specified feed. The working principle of the switch configuration is proven through simulation by representing it with a copper strip line. The presence of the copper strip shows that the switch is ON, and the absence of the copper represents OFF state condition. Moreover, the feed lines are designed in spiral geometry in order to avoid overlapping of different arms at its centre area. All four arms of R_1, R_2, R_3 and R_4 have a similar radius of 30 mm.

The top surface of the upper substrate consists of four radiating

elements denoted as R-A, R-B, R-C and R-D. As shown in Figure 2(b), the radiating elements with different sizes are positioned in a sequent spiral geometry. By having different sizes of the radiating element, with particular different slot positions and different lengths of the feed arm, the beam forming capability can be achieved while maintaining the operating frequency. While the bottom surface of upper substrate is free from copper.

Moreover, the proposed antenna uses four rectangular slots etched on the top surface of the lower substrate as constructed in Figure 2(a). The slots' width and length are determined as 14.4 mm × 1.25 mm respectively, evaluated based on equation in [16]. These slots are constructed 10 mm away from the edge of the rectangular radiating source (RRS) to maximize the power transfer to the radiator. Meanwhile, the lengths of RRS-1, RRS-2, RRS-3 and RRS-4 are set to 31 mm, 40 mm, 36 mm and 42 mm, respectively based on a few parametric studies.

Figure 3 shows photographs of the proposed antenna made of

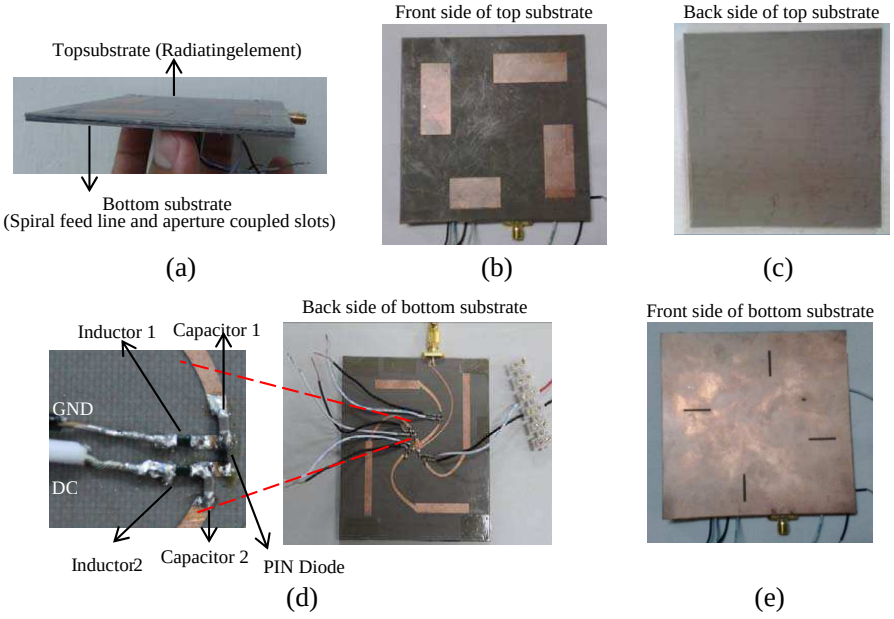

Figure 3. Photograph of the fabricated antenna. (a) Side view. (b) Radiating element. (c) Back side of top substrate. (d) Spiral feed line incorporates with RF PIN diode switches. (e) Rectangular aperture slots.

Taconic substrate with relative permittivity of 2.2 and loss tangent of 0.0009. Figures 3(b), 3(d) and 3(e) depict the radiating surface, aperture slot arrangement and feed line structure correspondingly. The feed line incorporates four PIN diode switches as shown in Figure 3(d). Each switch is developed from the surface mount component (SMC) and consists of one PIN diode, two capacitors, two inductors and a DC supply [17–20]. The capacitors will allow radio frequency (RF) signals to flow and block the DC simultaneously while the inductors allow the DC to flow and choke off the RF signals as well. Therefore, all DC flows in the other direction and ON the PIN diode. This complete circuit connection has ensured the RF signals to surge from the source feed to the radiating element.

A Programmable Intelligent Computer (PIC) microcontroller is connected to each of the switch through strip wires and powered up with a battery cell, as shown in Figure 4. The PIC board is developed with switch button and Light Emitting Diode (LED) highlighted by the yellow and red dotted lines, respectively. As the button is switched ON, the LED will turn ON, which indicates that the RF signals have flowed from the source feed to the radiating surface.

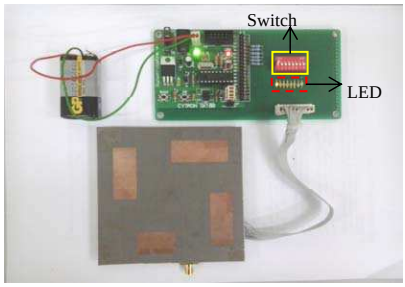

Figure 4. PIC microcontroller integration of the proposed antenna.

3. EXPERIMENTAL ANTENNA MEASUREMENT

The goal of the designed antenna is to achieve S_{11} less than -10 dB where 90% of power transmitted and 10% of power reflected. Therefore, instead of a proper antenna design, the selected Taconic substrate with electric loss tangent of 0.0009 helps to improve the antenna efficiency. Minimum tangent loss value gives the maximum electrical wave traveling through the substrate that fits for good conduction purpose as explained by Equation (1). The greater is the loss tangent, the superior is the attenuation of the electric field which makes the material suitable for electromagnetic absorption or shielding principle [21, 22]. Therefore, to prove this concept, the experimental

antenna measurement is focused on the return loss and radiation pattern parameter.

$$\tan\_\delta = \frac{\mu}{\varepsilon} \tag{1}$$

where

δ is loss tangent; wave attenuation level in the substrate.

μ is magnetic current rate in the substrate.

ε is electric current rate in the substrate.

3.1. Return Loss Result

An assembly of radiating element in an electrical and geometrical configuration will face a phenomenon called mutual coupling effect. Mutual coupling exists due to the interaction or coupling between the excited and isolated elements. It cannot be totally removed, but it can be minimized, depending on the separation distance between the elements. Such a scenario can be observed by the surface current distribution as illustrated in Figure 5. As switch A is ON in Figure 5(a), the current flows and excites the R-A with minimum mutual coupling effect. It can be observed in Figure 5(b) that the surface current only exists at R-B with switch B ON. Figures 5(c) and 5(d) depict the surface currents at R-C and R-D with switches C and D are ON, respectively. R-A and R-C have similar linear polarization at vertical axis. Meanwhile, R-B and R-D indicate horizontal linear polarization. It is clearly seen that the current is mainly distributed along the direction from the insert feed of $50\,\Omega$ SMA port to the radiating element. Therefore, the changes in current distribution lead to the reconfigurable beam pattern with certain switches configuration. Generally, the proposed antenna has good isolation with better efficiency of more than 65%.

As an EM wave travels from the source of the antenna to the *feed line*, *aperture slots*, *radiating element* and is excited in free space, the EM wave is encountered by a different impedance match at each interface. Therefore, the top and bottom substrates of the aperture coupled feed need to be aligned properly. Otherwise, some EM wave energy fraction will reflect back to the source and form a standing wave inside the feed line. The ratio of the maximum power to the minimum power is known as standing wave ratio (SWR). Ideally, SWR has a ratio of $1 : 1$.

This antenna has successfully achieved SWR of $2 : 1$ with a minimum reflection coefficient of less than $-10\,\mathrm{dB}$ ($S_{11} < -10\,\mathrm{dB}$). This indicates that 90% incident power is transmitted and only 10%

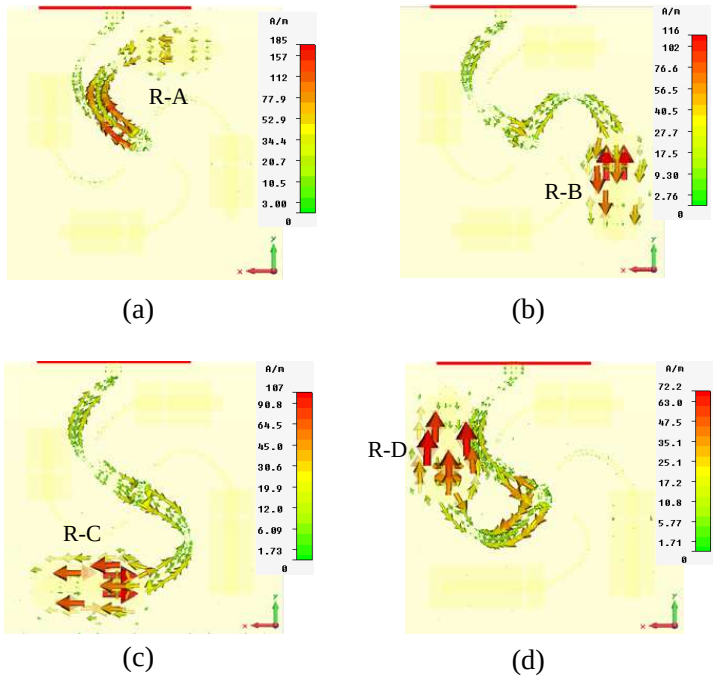

Figure 5. CST simulated electrical field results on the proposed antenna. (a) Switch A is ON. (b) Switch B is ON. (c) Switch C is ON. (d) Switch D is ON. The switches that not mentioned are in OFF state.

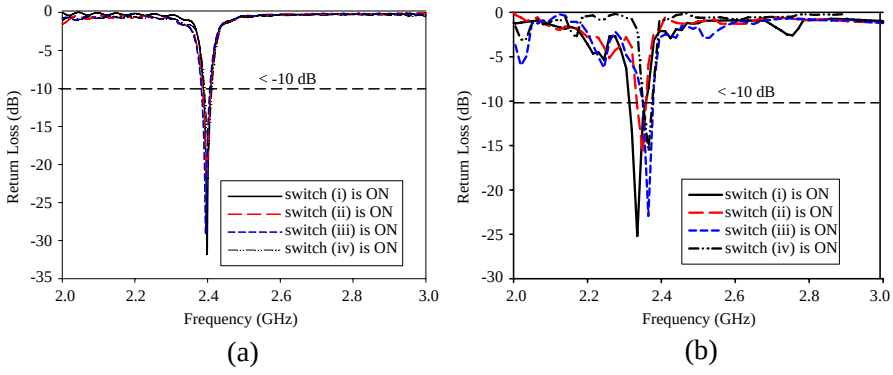

Figure 6. Simulated and measured return loss of the proposed antenna. (a) Simulated. (b) Measured.

reflected. All four switch configurations could operate within the range of 2.36 to 2.40 GHz as shown in Figure 6. Figures 6(a) and 6(b) depict simulated and measured return loss results, respectively. Regardless of switch configurations, the simulated return loss achieves resonance at 2.39 GHz with high impedance matching of nearly −35 dB. The measured return loss has slightly shifted to the lower frequency of 20 MHz with greater return loss than the simulation. The loss is due to the fabrication tolerance, material loss, subminiature (SMA) connector and inefficiency of PIC controller. However, these losses are still tolerable since the measured return loss is less than −10 dB.

3.2. Radiation Pattern Result

The radiation pattern measurement was performed in an Atenlab anechoic chamber as shown in Figure 7. The chamber helps to obtain optimum and realistic results by minimizing reflections during the measurement.

Figure 7. Radiation pattern measurement in the microwave anechoic chamber. (a) Point-to-point position. (b) Side view.

The antenna under test (AUT) acts as the transmitter and rotated 360 degrees in theta and phi axes to produce E-field and H-field radiation patterns. Meanwhile, a double ridged horn antenna is used as a dual polarization receiver. The line of sight (LOS) of both antennas is kept at 30 m. The AUT is connected to the first port of the PNA with an input power of 0 dBm, and the horn antenna is attached to the second port of the PNA. The PNA itself is connected to the computer via General Purpose Interface Bus (GPIB) cable. The Passive Measurement software will analyze and plot all the measured data such as gain, directivity and efficiency in 2D and 3D radiation pattern results.

Figure 8 shows the comparison results of the simulated and measured radiation patterns for each PIN diode switch configuration.

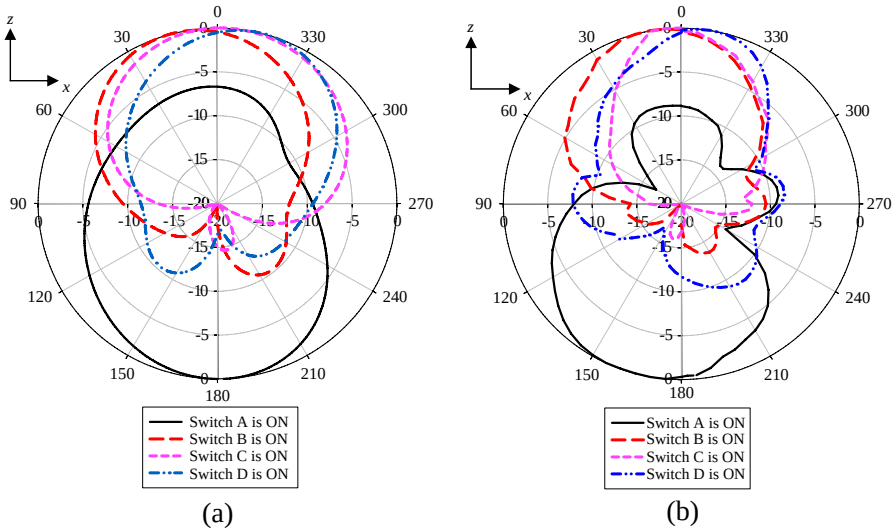

Figure 8. Simulated and measured polar radiation pattern of the proposed antenna. (a) Simulated. (b) Measured. The switches that not mentioned are in OFF state.

The polar graph results are normalized to their peak values as shown by the E-field pattern which is radiated on the z-x axis with the theta angle at resonant frequency of 2.39 GHz. Obviously, the proposed antenna achieves reconfigurable beam steering by controlling the PIN diode switches with the implementation of spiral feed arm design. Spiralling feed with the rectangular radiating element at the position of 0°, 90°, 180° and 360° contributes to the phase shift of the EM wave.

As summarized in Table 1, when switch A is ON with the other switches OFF, the antenna achieves radiation pattern at +176° with a gain of 2.81 dBi. By turning ON switch B, the main beam is steered to +10° with a gain of 4.2 dBi. When switch C is ON, the measurement shows that the proposed antenna directs the beam to −1° with optimum major lobe of 3.09 dBi as shown in Figure 8(b). As switch D is ON, the antenna demonstrates the radiation pattern of −12° with maximum beam of 3.89 dBi. The observation of measured polar patterns in Figure 8 shows the E-field pattern incurred shift in angles of about 2 to 4 degrees as well as the shape changes. The measurement indicates a bigger back lobe and side lobe beam than the simulation result, due to the diffraction contributed by the misalignment of upper and lower substrates, scattering effect of the cable and connector because they lie directly at the pattern cut [23–27].

Table 1. PIN diode switches configuration of the proposed beam steering antenna.

Type of Switch	Number of PIN diode switch	PIN diode status			
Reconfigurable RF PIN diode switches	A	ON	OFF	OFF	OFF
	B	OFF	ON	OFF	OFF
	C	OFF	OFF	ON	OFF
	D	OFF	OFF	OFF	ON
Simulated Angle of Steering Beam		+179°	+14°	−3°	−14°
Measured Angle of Steering Beam		+176°	+10°	−1°	−12°
Measured HPBW (°)		65° (195°–130°)	60° (340°–40°)	40° (340°–20°)	45° (330°–15°)
Measured Gain (dBi)		2.81	4.2	3.09	3.89

4. PRACTICAL ANTENNA MEASUREMENT

The outdoor practical measurement with varied points of received signal strength (RSS) is performed at Universiti Malaysia Perlis (UniMAP) as shown in Figure 9. The prototype test is carried out by taking 50 measurements within 5 m of distance at five different angles of +30°, +15°, 0°, −15° and −30°. Each of the angles is measured

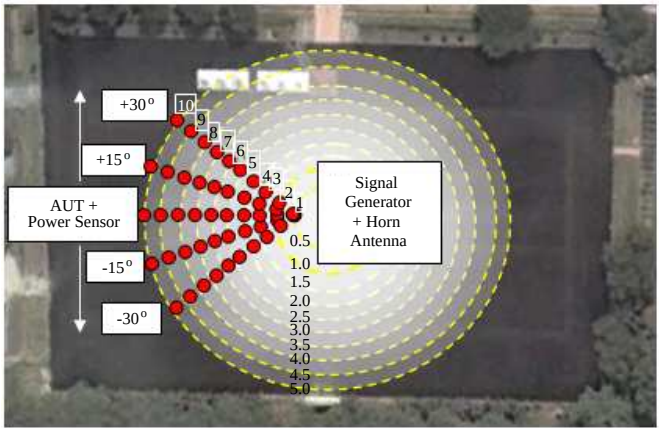

Figure 9. Measurement points at site testing of up to 5 m.

from point 1 to point 10 with variance of 0.5 m distance. Besides, it is ensured that no significant electromagnetical objects between the transmitter and the receiver.

The horn antenna connected to signal generator will transmit a 2.38 GHz signal to the proposed antenna. That beam forming antenna will detect the incoming signal accordingly with a certain PIN diode configuration controlled by the PIC microcontroller. This is realized by using U2002A (50 MHz–24 GHz) Agilent Power Sensor. It is a fast response device and a simple setup of plug and USB connectivity. Besides, the power measurement processes will be controlled by the Agilent Power Analysis software that manages to collect, analyze and display the data. Figure 10 shows the practical measurement setup.

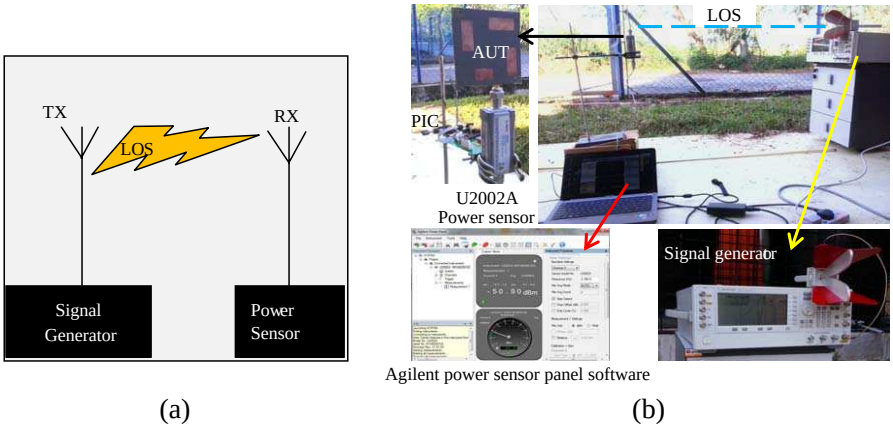

Figure 10. Measurement setup of power and distance. (a) Illustration. (b) On site measurement.

In order to be in the Fraunhofer region (far field), this research has kept the distance between the horn antenna and the AUT large enough and valid according to Equation (2) [28]. In the larger scale model, the signal strength propagation is influenced by reflection, diffraction and scattering effect. The propagation fading scenario can be classified in three cases; case 1 of path loss alone, case 2 of path loss and shadowing, case 3 of path loss, shadowing and multipath. However, this research only considers case 1 by aligning the transmitter antenna height until obtaining the maximum field strength at the AUT, which would then be able to minimize the multipath effect.

$$R = 2D^2/\lambda \tag{2}$$

where R is the separation distance of T_X and R_X, D the largest physical linear dimension of the antenna, and λ the signal wavelength.

Theoretically, the received signal strength over a large distance from the transmitter can be projected from Equation (2). In this research, the values of P_t, G_t, G_r, h_t, h_r and d are available. P_t is set to 0 dBm, and h_t and h_r are 0.5 m, while G_t and G_r are obtained from the data sheet and measured anechoic chamber result, respectively. The value of G_r is dependent on the degree of steering beam of 2.81 dBi, 4.2 dBi, 3.09 dBi and 3.89 dBi. Based on Equation (3), P_r is inversely proportional to the d value. Therefore, the signal strength reduces when travelling farther [1]

$$P_r = P_t G_t G_r \left(h_t^2 h_r^2 / d^4\right) \tag{3}$$

where P_r is the received power, G_t the gain of transmitting antenna (horn antenna), G_r the gain of receiving antenna (AUT), h_t the height of transmitting antenna, h_r the height of receiving antenna, and d the separation distance between the receiver and transmitter.

The measurement is carried out based on the PIN diode switch configuration as tabulated in Table 1. Consider beam steer 1 when switch A is ON while the others are OFF; beam steer 2, switch B is ON while others are OFF; beam steer 3 when switch C is ON while others are OFF and beam steer 4 when switch D is ON while others are OFF. Each beam steer is tested under line-of-sight (LOS) condition at 0° angle and non-line-of-sight (NLOS) at +30°, +15°, −15° and −30° angles over the 10 points of distance as illustrated in Figure 9. The difference in AUT gain according to beam steer conditions contributes to the different signal strengths at the same measurement point. This practical measurement is conducted to test and investigate the antenna functionality at 2.38 GHz frequency over various distance points and angles under the real field scenario.

Figure 11 shows that the LOS records better signal strength than all NLOS angles. For instance, Figure 11(a) shows the beam steer 1 with a gain of 2.81 dBi, which indicates a signal strength between −30 dBm to −48 dBm from point 1 to point 10 at angle of 0° angle. Among the NLOS measurements, the greater is the angle separation, the weaker is the power received. Therefore, it can be seen that +30° and −30° achieve a minimum power sensitivity of −57.15 dBm and −61.15 dBm.

For the beam steer 2, the NLOS measurement at +15 degrees yields the best result. This result proves the functionality of the designed antenna where the main beam is steered at +10 degrees. The better signal reception can be achieved since beam steer 2 is capable of tracking the transmitted signal with the main beam steered at 15°. At 30 degrees, the AUT is able to receive some considerable power compared to other angles, since the 10° coverage of the AUT with beam steer 2 is still able to receive signals from the signal generator.

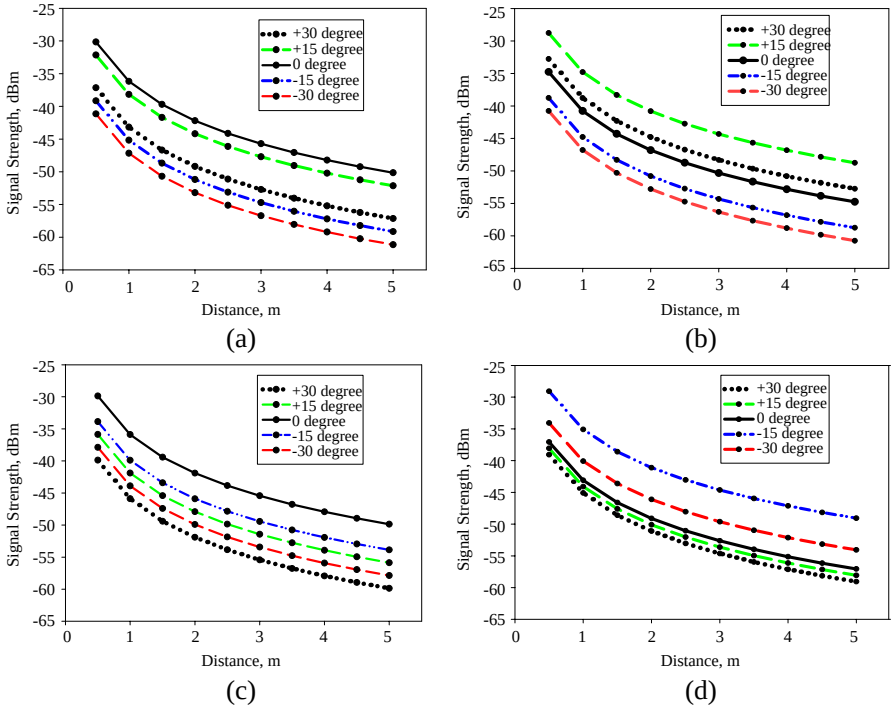

Figure 11. The signal strength of the reconfigurable beam steering antenna. (a) Beam steer 1. (b) Beam steer 2. (c) Beam steer 3. (d) Beam steer 4.

On the other hand, Figure 11(c) shows that the measurement at 0° records better signal reception than the measurements of other angles, because the main beam is almost steered to 0 degrees where the measurement yields that the main beam direction for beam steer 3 is at −1 degree. The remaining NLOS measurements yield expected result where the results indicate that the received power is less than the LOS measurement. Finally, Figure 11(d) depicts that the signal strength at −15 degrees achieves the best result where the main beam of the AUT is now directed at −10°. Overall, this section proves the beam steering functionality of the proposed antenna. Along with this unique feature, the proposed antenna is capable of maximizing the signal reception at the desired directions.

5. CONCLUSION

A novel design of a reconfigurable beam forming antenna with PIC microcontroller integration is introduced. It is realized by the aperture

coupled technique with a spiral feed method and differences of radiating element sizes in enhancing the beam steering performance. The reconfigurable beam is achieved with the integration of PIC microcontroller which is able to control the four sets of PIN diode switches. These four switches are positioned at specific locations of the proposed antenna spiral feed arm. With certain switch configurations, the proposed antenna is able to steer its radiating beam to four different angles of $+176^\circ$ $+10^\circ$, -1° and -12°. Moreover, the beam steers 1 and 2 are capable of radiating at a peak gain of 2.81 dBi and 4.2 dBi, respectively, while beam steers 3 and 4 achieve maximum beam radiations of 3.09 dBi and 3.89 dBi, respectively. Regardless of the switch configurations, the proposed antenna performs well at 2.39 GHz resonant with tolerable S_{11} of less than -10 dB. Furthermore, the on-site testing shows that four beams steering antenna has an average measured RSS with LOS of -30 dBm to -45 dBm, while for NLOS, each beam steering antenna has measured RSS range in between -35 dBm to -60 dBm. Besides, the antenna is fabricated on a compact Taconic substrate with a substrate dimension of 100 mm by 100 mm. It is proven by the measurement that the proposed antenna with numerous compensations is feasible for portable smart antenna of IEEE 802.16d fixed WiMAX, IEEE 802.16e mobile WiMAX and LTE applications.

REFERENCES

1. Rappaport, T. D., *Wireless Communication System,* 2nd Edition, John Wiley & Sons Inc., 2001.
2. Kang, W., K. H. Ko, and K. Kim, "A compact beam reconfigurable antenna for symmetric beam switching," *Progress In Electromagnetics Research*, Vol. 129, 1–16, 2012.
3. Peng, H.-L., W.-Y. Yin, J.-F. Mao, D. Huo, X. Hang, and L. Zhou, "A compact dual-polarized broadband antenna with hybrid beam-forming capabilities," *Progress In Electromagnetics Research*, Vol. 118, 253–271, 2011.
4. Liu, J., W.-Y. Yin, and S. He, "A new defected ground structure and its application for miniaturized switchable antenna," *Progress In Electromagnetics Research*, Vol. 107, 115–128, 2010.
5. Chen, J.-X., J. Shi, Z.-H. Bao, and Q. Xue, "Tunable and switchable bandpass filters using slot-line resonators," *Progress In Electromagnetics Research*, Vol. 111, 25–41, 2011.
6. Wounchoum, P., D. Worasawate, C. Phongcharoenpanich, and M. Krairiksh, "A switched-beam antenna using circumferential-

slots on a concentric sectoral cylindrical cavity excited by coupling slots," *Progress In Electromagnetics Research*, Vol. 120, 127–141, 2011.

7. Venneri, F., S. Costanzo, and G. Di Massa, "Transmission line analysis of aperture-coupled reflect arrays," *Progress In Electromagnetics Research C*, Vol. 4, 1–12, 2008.
8. Li, G., S. Yang, Y. Chen, and Z.-P. Nie, "A novel electronic beam steering technique in time modulated antenna array," *Progress In Electromagnetics Research*, Vol. 97, 391–405, 2009.
9. Jung, Y.-B., A. V. Shishlov, and S.-O. Park, "Cassegrain antenna with hybrid beam steering scheme for mobile satellite communications," *IEEE Transactions on Antennas and Propagation*, Vol. 57, No. 5, May 2009.
10. Ouyang, J., F. Yang, S. W. Yang, Z. P. Nie, and Z. Q. Zhao, "A novel radiation pattern and frequency reconfigurable microstrip antenna on a thin substrate for wide-band and wide-angle scanning application," *Progress In Electromagnetics Research Letters*, Vol. 4, 167–172, 2008.
11. Sanada, A. and D. Taema, "A Ka-band low-profile beam steering slot antenna using a CRLH substrate integrated waveguide," *European Conference in Antennas and Propagation, EuCAP 2009*, 611–614, 2009.
12. Shynu Nair, S. V. and M. J. Ammann, "Reconfigurable antenna with elevation and azimuth beam switching," *IEEE Antennas and Wireless Propagation Letters*, Vol. 9, 367–370, 2010.
13. Fayad, H. and P. Record, "Multi-feed dielectric resonator antenna with reconfigurable radiation pattern," *Progress In Electromagnetics Research*, Vol. 76, 341–356, 2007.
14. Mofolo, M., A. Lysko, and W. Clarke, "A method of electronic beam steering for circular switched parasitic dipole arrays," *Southern Africa Telecommunication Networks and Applications Conference, SATNAC 2010*, 6, 2010.
15. Monti, G., L. Corchia, and L. Tarricone, "Patch antenna with reconfiguration polarization," *Progress In Electromagnetics Research C*, Vol. 9, 13–23, 2009.
16. Maloney, J. C., M. P. Kesler, L. M. Lust, L. N. Pringle, T. L. Fountain, and P. H. harms, "Switched fragmented aperture antennas," *Proc. IEEE Antennas Propagat. Soc. Int. Symp.*, Vol. 1, 310–313, 2000.
17. Jamlos, M. F., T. A. Rahman, M. R. Kamarudin, P. Saad, O. A. Aziz, and M. A. Shamsudin, "Adaptive beam steering of RLSA antenna with RFID technology," *Progress In Electromag-*

netics Research, Vol. 108, 65–80, 2010.

18. Jusoh, M., M. F. Jamlos, M. R. Kamarudin, F. Malek, M. A. Romli, Z. A. Ahmad, M. H. Mat, and M. S. Zulkiflie, "A reconfigurable ultra-wideband (UWB) compact tree-design antenna system," *Progress In Electromagnetic and Research C*, Vol. 30, 131–145, 2012.
19. Jamlos, M. F., O. A. Aziz, T. A. Rahman, M. R. Kamarudin, P. Saad, M. T. Ali, and M. N. Md Tan, "A reconfigurable radial line slot array (RLSA) antenna for beam shape and broadside application," *Journal of Electromagnetic Waves and Applications*, Vol. 24, Nos. 8–9, 1171–1182, 2010.
20. Ali, M. T., M. N. Md Tan, T. A. Rahman, M. R. Kamarudin, M. F. B. Jamlos, and R. Sauleau, "A novel of reconfigurable planar antenna array (RPAA) with beam steering control," *Progress In Electromagnetics Research B*, Vol. 20, 125–146, 2010.
21. Emerson & Cuming, "Theory and application of RF/microwave absorbers," http://www.eccosorb.com/resource-white-papers.htm/.
22. Iqbal, M. N., M. F. B. A. Malek, S. H. Ronald, M. S. Bin Mezan, K. M. Juni, and R. Chat, "A study of the EMC performance of a graded-impedance, microwave, risk-husk absorber," *Progress In Electromagnetics Research*, Vol. 131, 19–44, 2012.
23. Wee, F. H., M. F. B. A. Malek, S. Sreekantan, A. U. Al-Amani, F. Ghani, and K. Y. You, "Investigation of the characteristics of barium strontium titanate (BST) dielectric resonator ceramic loaded on array antennas," *Progress In Electromagnetics Research*, Vol. 121, 181–213, 2011.
24. Hashim, A. M., "Development of microstrip patch array antenna wireless local area network (WLAN)," *ETRI Journal*, Vol. 35, No. 5, Oct. 2010.
25. Zubir, F., M. K. A. Rahim, O. B. Ayop, and H. A. Majid, "Design and analysis of microstrip reflect array antenna with Minkowski shape radiating element," *Progress In Electromagnetics Research B*, Vol. 24, 317–331, 2010.
26. Tze-Meng, O., K. G. Tan, and A. W. Reza, "A dual-band omnidirectional microstrip antenna," *Progress In Electromagnetics Research*, Vol. 106, 363–376, 2010.
27. Mazinani, S. M. and H. R. Hassani, "A novel omnidirectional broadband planar monopole antenna with various loading plate shapes," *Progress In Electromagnetics Research*, Vol. 97, 241–257, 2009.
28. Constantine, B. A., *Antenna Theory, Analysis and Design,* 3rd edition, John Wiley & Sons, 2005.